Numerical study on sequential period-doubling bifurcations of graphene wrinkles on a soft substrate

Jong Hyun Jung[a], Jaehyun Bae[a], Myoung-Woon Moon[b], Kyung-Suk Kim[c], Jisoon Ihm[a,*]

[a] *Department of Physics and Astronomy, Seoul National University, Seoul 151-747, Republic of Korea*
[b] *Korea Institute of Science and Technology, Seoul 136-791, Republic of Korea*
[c] *School of Engineering, Brown University, Providence, Rhode Island 02912, USA*

Abstract

A compressed stiff film on a soft substrate may exhibit wrinkles and, under increased compressive strain, post-buckling instabilities as well. We numerically analyze wrinkling behaviors of graphene attached on a polydimethylsiloxane (PDMS) substrate under lateral compression. The finite element method is used to simulate the equilibrium shape of the wrinkles as a function of compressive strain. Two-dimensional stretching and bending properties of graphene are obtained by density functional theory analysis, which are then converted to equivalent elastic properties of a continuum film with finite effective thickness. The PDMS is described using an Ogden or a neo-Hookean material model. Wrinkles first appear at extremely small strain. As the lateral compression increases, due to the nonlinear elasticity of the PDMS, sequential period-doubling bifurcations of the wrinkle mode are activated until the bifurcation stops and the film folds. We show that the bifurcations are consequences of a delicate balance between the deformations of the film and the substrate to minimize the total energy.

Keywords: A. Graphene, C. Wrinkle, D. Bifurcation, D. Period-doubling

*Corresponding author
Email address: jihm@snu.ac.kr (Jisoon Ihm)

1. Introduction

Wrinkles on material surfaces have generated considerable research interest these days. They are common in nature as exemplified by skin wrinkles and geological folds [1, 2]. Wrinkles are also formed when a stiff film on a compliant substrate is compressed laterally [3–6]. They have been used to fabricate stretchable electronics [7].

When the wrinkles are further compressed, post-buckling instability may occur and complex patterns can arise. Suppose sinusoidal wrinkles originally exist on a stiff film. For an increased compression, another mode of the sinusoidal wrinkle whose wavelength is twice the initial value couples to the original one. Such spatial period doubling has been found in experiment and attributed to the quadratic and cubic nonlinear elasticity of the film and the substrate [8–13]. Further compression leads to a period-quadrupling bifurcation [8, 14]. These phenomena suggest that continued increase in compression may lead to repeated bifurcations and such sequential period-doubling bifurcations in some systems show a transition to chaos [15–17]. In the present work, we choose graphene on a polydimethylsiloxane (PDMS) substrate as a model system [18–20]. Sequential period-doubling bifurcations up to octupling will be shown to occur in the Ogden model. We will further demonstrate that the wrinkles will be folded, namely, two side walls of a valley will touch each other, the bifurcation will stop, and the system will not proceed to chaos.

2. Methods

Now, the behavior of wrinkles on a single-layer graphene attached on a PDMS substrate was studied numerically using the finite element method (FEM). Such a numerical approach was unavoidable because the governing equations of the finite deformation are nonlinear partial differential equations which do not allow for analytic solutions. Our calculation was based on the method of Sun *et al.* [11, 12]. One-dimensional wrinkles were considered, and the plane strain approximation was used. To perform the FEM calculations, some physical param-

eters of the system were required. We carried out *ab initio* electronic structure calculations based on the density functional theory (DFT) with the Perdew-Burke-Ernzerhof (PBE) exchange-correlation functional [21] using the Vienna *ab initio* simulation package (VASP) [22]. We employed the projector-augmented wave (PAW) pseudopotential [23]. From these calculations, we obtained bending modulus $D = 1.5$ eV and in-plane 2-dimensional modulus $E^{2\mathrm{D}} = 2000$ eV/nm^2. Graphene's Poisson's ratio, $\nu = 0.15$, was chosen from the literature [24]. In order to apply these pieces of information to the well-established formalism of the wrinkle formation, [12] we needed to convert D and $E^{2\mathrm{D}}$ into the 3-dimensional E and the "effective" thickness of the film, h. From the relation $E^{2\mathrm{D}} = Eh$ and $D = Eh^3/12(1-\nu^2)$, we obtained the "effective" thickness $h = 0.094$ nm and the "effective" Young's modulus $E = 3.4$ TPa. The above procedure amounts to converting the single-layer graphene to a continuum plate. Now, in extracting the material properties of the substrate (PDMS), its elastic response was approximated by two different models, the Ogden and the neo-Hookean models. The Ogden model shows material stiffening at high strain compared to an almost linear response in the neo-Hookean model in Fig. 1. In the Ogden model, [25] the second order incompressible strain energy potential was defined as

$$U(\lambda_1, \lambda_2, \lambda_3) = \sum_{i=1}^{2} \frac{2\mu_i}{\alpha_i^2}(\lambda_1^{\alpha_i} + \lambda_2^{\alpha_i} + \lambda_3^{\alpha_i} - 3), \tag{1}$$

where λ_i's are the principal stretches, and μ_i's and α_i's are material constants related to the strain energy. The principal stretches λ_i's are defined as the eigenvalues of $\sqrt{\mathbf{F}^T\mathbf{F}}$, where $\mathbf{F}$ is the deformation gradient defined as $F_{iI} = \partial x_i/\partial X_I$ $(i, I = 1, 2, 3)$, where X_I and x_i are the coordinates of a point in the material in the undeformed and deformed configuration, respectively. We fitted the potential to the stress-strain curve of PDMS [26] and obtained $\mu_1 = 0.7526$ MPa, $\mu_2 = 0.0388$ MPa, $\alpha_1 = 1.301$, and $\alpha_2 = 11.39$ (Fig. 1). The summation index i ran to 2 because two terms were necessary to fit the curve where the nominal strain ranged between 0 and 0.85. The compressive nominal strain is defined as $\epsilon = (L_0 - L_\mathrm{c})/L_0$ with the initial sample length L_0 and the compressed length L_c.

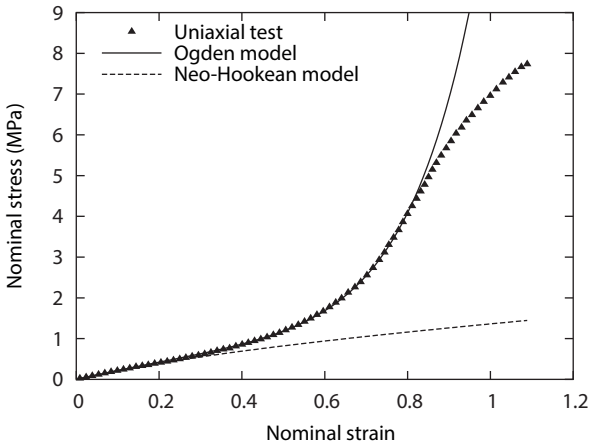

Figure 1: Fitting of the measured stress-strain curve of the PDMS substrate with theoretical models. The measured data were reprinted with permission from Choi *et al.*, Exp. Mech. **50**, 635 (2010). Copyright 2010 Springer.

The FEM calculation was done using the ABAQUS 6.12 standard code [27]. The film was described by quadratic beam elements with the hybrid formulation (B22H) and the substrate by the hybrid quadrilateral elements (CPE8RH) [11, 12]. To break the translational symmetry of the system and trigger wrinkling, a small sinusoidal displacement with an anticipated wavelength on the film was introduced. The amplitude of the sinusoidal displacement was as small as $0.05h$. The anticipated wavelength of the wrinkle was obtained from the following equation, [12]

$$L = \frac{2\pi h}{\lambda}\left(\frac{E}{6(1+\lambda^2)Q(1-\nu^2)}\right)^{1/3} \approx 2\pi\left(\frac{D}{Q}\right)^{1/3}, \tag{2}$$

where λ, the principal stretch in the direction of compression, was close to 1 in practice, and Q was the shear modulus in the small strain limit ($= 0.791$ MPa for PDMS [26]). To induce bifurcations, a numerical technique of introducing an artificial damping factor for computational stabilization was used. The artificial damping was applied to enhance convergence at bifurcations. The undesired artifact of the damping was minimized by optimizing it to the smallest possible value so that it reproduced the experimentally observed and previously

calculated period doubling and quadrupling [8, 11, 14]. We imposed additional boundary conditions in which tangent lines of the film on each end were kept horizontal (cantilever beam conditions). The horizontal length and depth of the substrate were 24 and 5 times of the wavelength of the wrinkle mode, respectively. We checked and confirmed that the length and depth of the substrate were sufficient to prevent artificial interactions between top and bottom parts of the system.

3. Results and Discussion

Development of the wrinkled surface morphology of monolayer graphene on PDMS is shown as a function of the compressive strain in Fig. 2. The contour plots display the maximum in-plane principal logarithmic strain, which is defined as the largest eigenvalue of the logarithmic strain tensor $\mathbf{E_l}$. This tensor is a measure of finite deformation which is defined as $\mathbf{E_l} = \ln\sqrt{\mathbf{F}^T\mathbf{F}}$. The wrinkle generally starts at a particular finite strain value. However, the critical strain for the onset of wrinkle formation is so tiny [12] (4.9×10^{-5}) that it is not noticeable in the figure. Initially, the wavelength of the wrinkle in Fig. 2(a1) is 42.2 nm (Eq. (2)). After the wrinkle forms, the amplitude of the sinusoidal wrinkle increases as the magnitude of the compressive strain increases. When the compressive strain exceeds 0.16, a bifurcation (known as pitchfork bifurcation) sets in with a period doubling as described in Fig. 2(a2). The critical ϵ for the onset of the period doubling agrees reasonably with previous results ($\epsilon = 0.185$) found in the literature [10, 11]. A further compression induces a period quadrupling (a3) with its shape also in good agreement with previous results [8, 14]. A larger strain induces the period octupling. At a slightly greater ϵ, the folding finally occurs. Here, the term "fold" is defined as a wrinkle developed so deeply that two side walls of the sink touch each other. The fold exhibits a concave valley whose depth in the vertical direction increases with compression. The maximum of the local strain E_{11} ($= \partial u_1/\partial X_1$, where $u_1 = x_1 - X_1$) of graphene is estimated to be 0.031 at the bottom of the valley,

which is still much less than the measured intrinsic fracture strain of graphene (0.25) [28]. This value is also smaller than the failure strain (0.087) of a defected carbon nanotube reported in the literature [29]. Therefore, the folded graphene is unlikely to be broken under the nominal compressive strain as large as 0.34.

Another instructive way of examining the repeated bifurcations is presented in Fig. 2(b). Here, the development of the surface height (y-coordinate) variations at different positions (marked with arrows of different colors) is traced as ϵ increases. At the period-doubling bifurcation ($\epsilon = 0.16$), the y-coordinate of the valley at the red arrow position swells while the other three valleys (black, blue, and green arrow positions) deepen [8]. When the strain increases beyond 0.24, a bifurcation takes place again and the valley at the black arrow position goes up while those at blue and green arrow positions deepen. At $\epsilon = 0.27$, another bifurcation with period octupling is observed. Then at $\epsilon = 0.29$, two side walls of a valley touch each other, namely, the film folds.

Now, we analyze various components of the energy at different stages of conformation. The dimensionless substrate energy change relative to the flat substrate, $\Delta U^{\mathrm{s}} = (U^{\mathrm{s}}_{\mathrm{w}} - U^{\mathrm{s}}_{0})(1-\nu_{\mathrm{s}}^2)/ALE_{\mathrm{s}}$, as a function of ϵ is plotted in Fig. 2(c), where $U^{\mathrm{s}}_{\mathrm{w}}$ is the wrinkled substrate energy, U^{s} is the energy of the flat substrate under the same ϵ, ν_{s} (≈ 0.5) is the Poisson's ratio of the substrate, A is the area of the film surface, and E_{s} ($= 3Q$) is the modulus of the substrate. At $\epsilon = 0.16$, $\mathrm{d}\Delta U^{\mathrm{s}}/\mathrm{d}\epsilon$ increases discontinuously indicating the onset of period doubling. The energy derivative increases because the period doubling mode causes more deformation of the substrate. The bifurcation is energetically unfavorable for the substrate. A similar phenomenon occurs at $\epsilon = 0.24$ as the period quadrupling starts. At $\epsilon = 0.27$ or greater, the behavior of the energy derivative is rather intricate. We conjecture that the simulation becomes numerically less stable when the conformation gets complicated (period octupling at $\epsilon \approx 0.27$ and folding at $\epsilon \approx 0.29$). The dimensionless film energy change $U^{\mathrm{f}} = U^{\mathrm{f}}_{\mathrm{w}}(1-\nu_{\mathrm{s}}^2)/ALE_{\mathrm{s}}$ is also shown in Fig. 2(c), where $U^{\mathrm{f}}_{\mathrm{w}}$ is the wrinkled film energy. The energy derivative $\mathrm{d}U^{\mathrm{f}}/\mathrm{d}\epsilon$ decreases abruptly at the bifurcation points implying that the bifurcations should be energetically favorable to the

film. The sum of the two differentiated energies, $\mathrm{d}(\Delta U^{\mathrm{s}} + U^{\mathrm{f}})/\mathrm{d}\epsilon$ has kinks and is almost continuous at the bifurcation points in line with a previous work [8]. In the literature, the period doubling bifurcation was attributed to non-negligible second-order terms in the strain tensor (so-called geometric nonlinearity) for a large deformation as well as the nonlinear elasticity in the constitutive equation of the substrate [9, 10]. There, it was shown that the period doubling mode reduced the total energy. In our analysis, we have shown in detail that period doubling and quadrupling bifurcations release the film energy more at the expense of smaller increase in the substrate energy. Parenthetically, we want to note that the sequential period doubling bifurcations in nonlinear systems may lead to chaos [3, 15, 16]. Before this happens, the ratio of successive bifurcation intervals $\delta_n = (\epsilon_{n+1} - \epsilon_n)/(\epsilon_{n+2} - \epsilon_{n+1})$ usually converges to the Feigenbaum constant $\delta = 4.66\ldots$ as n increases [17]. In our system, $\delta_1 = 3.8$. It is conceivable that, if the contact between the wrinkles (folding) did not happen, a further compression might lead to chaos in our system.

To separate out the effect of the stiffening of the PDMS substrate at large strain, calculations with the neo-Hookean model (free of stiffening) were also carried out in place of the Ogden model. In the neo-Hookean model, the period doubling and quadrupling were observed at $\epsilon = 0.19$, and 0.26 (Fig. 3), similar to the Ogden model. However, as the strain increased, a particular valley of the wrinkle structure was deepened (the green dash-dot arrow) and neighboring valleys were flattened (the blue solid and black dashed arrows) [30, 31]. This is because the material in the neo-Hookean model does not stiffen as much as in the Ogden model at large strain, thereby admitting for a large deformation of the deep wrinkle. The strain at the deep valleys calculated by the Ogden model exceeds 0.5 (Fig. 2(a5)). At this large strain, the neo-Hookean model stiffens less than the Ogden model does as shown in Fig. 1. In the neo-Hookean model, the bifurcations proceed to quadrupling followed by folding and subsequent localization of the fold, without octupling.

4. Conclusions

In summary, we have demonstrated numerically that consecutive period-doubling bifurcations take place in the wrinkles of graphene (a stiff film) attached on the PDMS (a soft substrate). It is shown that the bifurcations arise because they reduce the energy of the film more at the expense of a smaller increase in the substrate energy. Eventually, folding of the wrinkles occurs, and thus bifurcation stops. We expect that the result obtained here regarding the folding of the wrinkled film can be applied to the fabrication of nano channels and externally controlling the conformation of such channels by changing the strain.

Acknowledgments

JHJ, JB, and JI were supported by the National Research Foundation of Korea through the MSIP Grant No. 2006-0093853 and the Korea Institute of Science and Technology. MWM was supported by the Korea Institute of Science and Technology (KIST), and KSK by the Institute for Molecular and Nanoscale Innovation (IMNI) at Brown University (GR260000.1001) and KIST (529243). Computations were performed through the support of the Korea Institute of Science and Technology Information.

References

[1] K. Efimenko, M. Rackaitis, E. Manias, A. Vaziri, L. Mahadevan, J. Genzer, Nat. Mater. 4 (2005) 293–7. doi:10.1038/nmat1342.

[2] P. J. Hudleston, S. H. Treagus, J. Struct. Geol. 32 (2010) 2042–71. doi:10.1016/j.jsg.2010.08.011.

[3] F. Brau, P. Damman, H. Diamant, T. A. Witten, Soft Matter 9 (2013) 8177–86. doi:10.1039/C3SM50655J.

[4] B. Li, Y.-P. Cao, X.-Q. Feng, H. Gao, Soft Matter 8 (2012) 5728–45. doi:10.1039/C2SM00011C.

[5] E. Cerda, L. Mahadevan, Phys. Rev. Lett. 90 (2003) 074302. doi:10.1103/PhysRevLett.90.074302.

[6] Z. Huang, W. Hong, Z. Suo, Phys. Rev. E 70 (2004) 030601(R). doi:10.1103/PhysRevE.70.030601.

[7] M. Kaltenbrunner, T. Sekitani, J. Reeder, T. Yokota, K. Kuribara, T. Tokuhara, M. Drack, R. Schwödiauer, I. Graz, S. Bauer-Gogonea, S. Bauer, T. Someya, Nature 499 (2013) 458–63. doi:10.1038/nature12314.

[8] F. Brau, H. Vandeparre, A. Sabbah, C. Poulard, A. Boudaoud, P. Damman, Nat. Phys. 7 (2011) 56–60. doi:10.1038/nphys1806.

[9] L. Zhuo, Y. Zhang, Int. J. Solids Struct. 53 (2015) 28–37. doi:10.1016/j.ijsolstr.2014.10.028.

[10] Y. Zhao, Y. Cao, W. Hong, M. K. Wadee, X.-Q. Feng, Proc. R. Soc. A 471 (2015) 20140695. doi:10.1098/rspa.2014.0695.

[11] Y. Cao, J. W. Hutchinson, J. Appl. Mech. 79 (2012) 031019. doi:10.1115/1.4005960.

[12] J.-Y. Sun, S. Xia, M.-W. Moon, K. H. Oh, K.-S. Kim, Proc. R. Soc. A 468 (2012) 932–53.

[13] Q. Wang, X. Zhao, Sci. Rep. 5 (2015) 8887.

[14] B. Li, Y.-P. Cao, X.-Q. Feng, H. Gao, J. Mech. Phys. Solids 59 (2011) 758–74.

[15] E. Sander, J. A. Yorke, Int. J. Bifurcation Chaos Appl. Sci. Eng. 22 (2012) 1250022. doi:10.1142/S0218127412500228.

[16] M. J. Feigenbaum, J. Stat. Phys. 19 (1978) 25–52.

[17] P. Cvitanovic, Universality in Chaos, Bristol: Adam Hilger, 1984. P. 28.

[18] S. Scharfenberg, D. Z. Rocklin, C. Chialvo, R. L. Weaver, P. M. Goldbart, N. Mason, App. Phys. Lett. 98 (2011) 091908. doi:10.1063/1.3553228.

[19] S. Scharfenberg, N. Mansukhani, C. Chialvo, R. L. Weaver, N. Mason, App. Phys. Lett. 100 (2012) 021910. doi:10.1063/1.3676059.

[20] Z. Zhang, T. Li, J. Appl. Phys. 110 (2011) 083526. doi:10.1063/1.3656720.

[21] J. P. Perdew, K. Burke, M. Ernzerhof, Phys. Rev. Lett. 77 (1996) 3865–8. doi:10.1103/PhysRevLett.77.3865.

[22] G. Kresse, J. Furthmüller, Phys. Rev. B 54 (1996) 11169.

[23] G. Kresse, D. Joubert, Phys. Rev. B 59 (1999) 1758–75.

[24] K. N. Kudin, G. E. Scuseria, B. I. Yakobson, Phys. Rev. B 64 (2001) 235406. doi:10.1103/PhysRevB.64.235406.

[25] R. W. Ogden, Proc. R. Soc. London, Ser. A 326 (1972) 565–84. doi:10.1098/rspa.1972.0026.

[26] H.-J. Choi, J.-H. Kim, H.-J. Lee, S.-A. Song, H.-J. Lee, J.-H. Han, M.-W. Moon, Exp. Mech. 50 (2010) 635–41.

[27] ABAQUS 6.12 Documentation Collection, Dassault Systèmes, Providence, RI, 2012.

[28] C. Lee, X. Wei, J. W. Kysar, J. Hone, Science 321 (2008) 385–8.

[29] S. L. Mielke, D. Troya, S. Zhang, J.-L. Li, S. Xiao, R. Car, R. S. Ruoff, G. C. Schatz, T. Belytschko, Chem. Phys. Lett 390 (2004) 413–20.

[30] Y. Cao, J. W. Hutchinson, Proc. R. Soc. A 468 (2012) 94–115.

[31] L. Pocivavsek, R. Dellsy, A. Kern, S. Johnson, B. Lin, K. Y. C. Lee, E. Cerda, Science 320 (2008) 912–6. doi:10.1126/science.1154069.

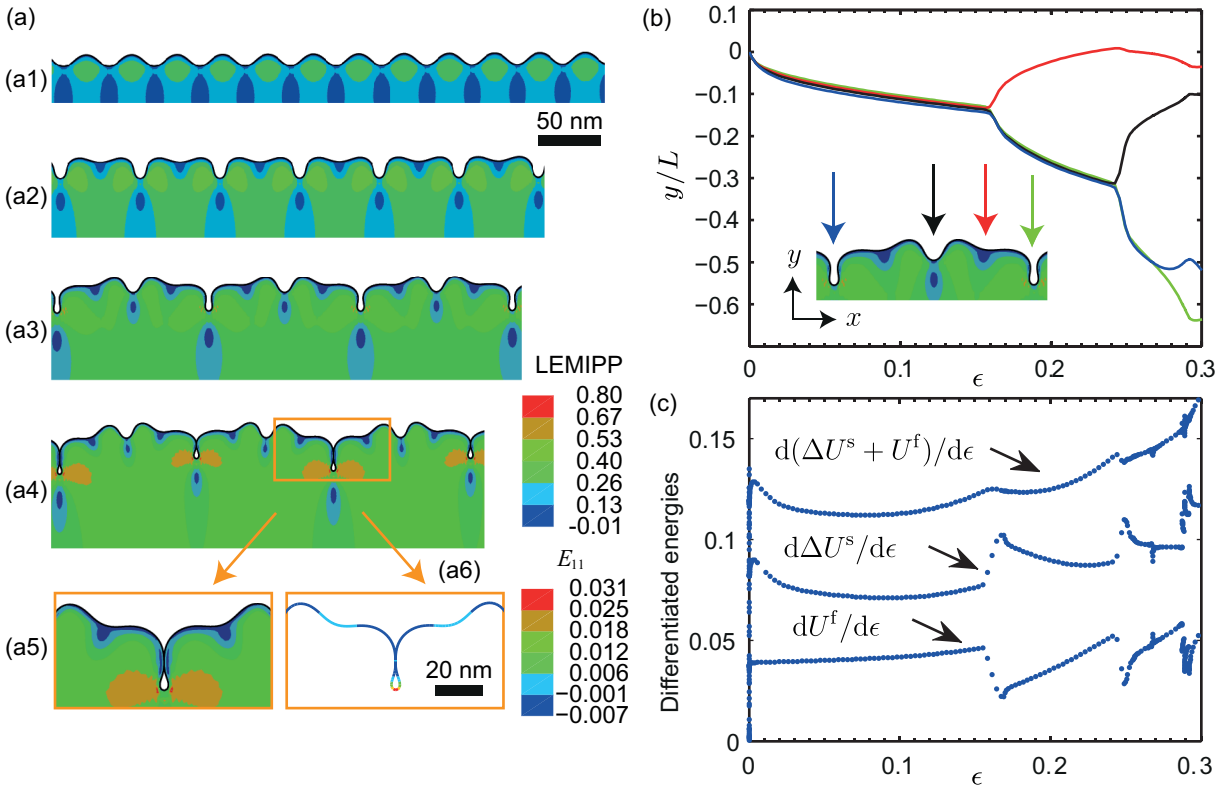

Figure 2: (a1–a4) Buckled surface configurations with the Ogden model substrate at compressive strain $\epsilon = 0.13$, 0.23, 0.26 and 0.34, respectively. At high strain of 0.34, a magnified picture (a5) shows the graphene fold with two side walls contacting each other. LEMIPP means the maximum in-plane principal logarithmic strain. The color code (a6) shows the local strain E_{11} as defined in the text. (b) Calculated y-directional displacement of 4 different points (indicated with 4 arrows) on the surface at the bottom of valleys as a function of compressive strain ϵ from our calculation. Three different bifurcation points are identified at the strain of 0.16, 0.25, and 0.27, respectively. (c) Nondimensionalized energy derivatives as defined in the text as a function of compressive strain ϵ.

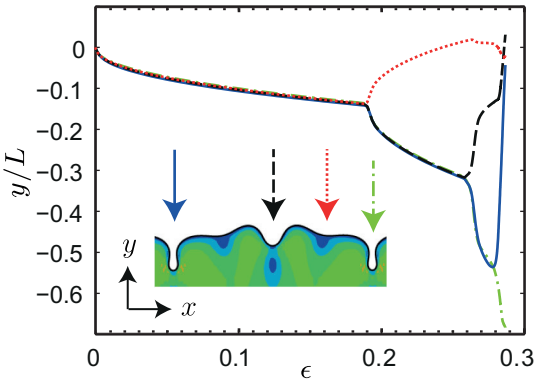

Figure 3: y-directional displacement of 4 different points (indicated with 4 arrows) on the surface at the bottom of valleys as a function of strain calculated with the neo-Hookean model for the substrate. Two different bifurcation points are identified at the strain of 0.19, 0.26, respectively. The last separation of lines at $\epsilon \approx 0.28$ corresponds to the deepening of one valley (at the green dash-dot arrow) and the flattening of neighboring valleys.